JOURNAL OF CATALYSIS 76, 112–132 (1982)

Infrared and Mössbauer Spectroscopic Studies of the Interaction of Nitric Oxide with Fe–Y Zeolite

KOH-ICHI SEGAWA,* YI CHEN,†,[1] JOSEPH E. KUBSH,† W. N. DELGASS,†,[2] J. A. DUMESIC,†,[3] AND W. KEITH HALL*

Laboratory for Surface Studies, Department of Chemistry, University of Wisconsin, Milwaukee, Wisconsin 53201, and †Department of Chemical Engineering, University of Wisconsin, Madison, Wisconsin 53706

Received November 23, 1981; revised February 19, 1982

The time evolution of infrared spectra obtained from NO adsorbed on reduced Fe–Y zeolite at room temperature is reported. Bands near 1845 and 1870 cm^{-1} formed quickly and remained invariant while bands at 1917 and 1815 cm^{-1} grew slowly over periods of hours. The intensity ratio of the latter two bands remained constant during growth and decay, and they were therefore attributed to a dinitrosyl species formed within the supercages. On evacuation at room temperature, the dinitrosyl species was converted to a mononitrosyl species with an absorption band at 1767 cm^{-1}. All bands disappeared on evacuation above 520 K. The dinitrosyl bands also disappeared on heating in NO but the absorption in the region 1855 to 1870 cm^{-1} did not, showing that the oxidized form of this material chemisorbed NO, presumably as a mononitrosyl species. The ir bands characteristic of NO adsorbed on reduced Fe–Y were also eliminated by exposure of the sample to O_2 at room temperature. In both of these cases, however, the extent of NO adsorption on oxidized Fe–Y zeolite was significantly smaller than that on reduced Fe–Y. Gravimetric studies showed that the total adsorption of NO grew slowly over a period of 20 h at room temperature to a value more than twice its initial value. This corresponded to the formation of increasing amounts of the dinitrosyl species. The data suggested that new sites were being formed in the supercages concomitant with the slow diffusion of iron to an accessible location. Mössbauer spectroscopy was used to probe those sites in the zeolite structure responsible for the different nitrosyl complexes observed in the infrared spectra. Reduced Fe–Y zeolite showed two Fe^{2+} doublets due to iron cations of different coordination. Upon exposure to NO at room temperature, those Fe^{2+} cations of low coordination which were accessible to gases (at Sites II and II′) formed nitrosyl complexes. The infrared bands at 1845 and 1870 cm^{-1} are assigned to these complexes. Ferrous cations of high coordination (presumably at Site I) also formed nitrosyl complexes by migrating to sites of high accessibility. The dinitrosyl bands are assigned to these complexes. The mononitrosyl species at 1767 cm^{-1}, which was formed from the dinitrosyl species upon evacuation, gave rise to a Mössbauer spectrum characteristic of highly coordinated iron. It is suggested that this low-frequency mononitrosyl species is due to NO adsorbed on iron cations at Site III′ in the supercages.

INTRODUCTION

Some time ago it was found that Fe–Y zeolite could be oxidized and reduced reversibly with O_2 and H_2, respectively, between the valence states Fe^{2+} and Fe^{3+} (*1*). Thus, the zeolite acted as an oxygen carrier with a capacity O/Fe = 0.5. More recently, Fu *et al.* (*2*) showed that NO and N_2O could be used as oxidizing agents instead of O_2 and that CO worked equally as a reducing agent. Moreover, since the two steps could be carried out separately, they could be carried out together and the zeolite then acted effectively as an NO_x catalyst.

Two kinds of models for the redox site are immediately apparent. Evidence may be advanced in support of each, and each has features which are difficult to understand. The first model is based on an oxygen atom carrier. A site is oxidized when an O atom is deposited by the oxidizing agent,

---

[1] Visiting scholar from the Department of Chemistry, Nanking University, Peoples' Republic of China.

[2] Permanent address: Department of Chemical Engineering, Purdue University, West Lafayette, Ind. 47907.

[3] To whom all correspondence should be sent.

0021-9517/82/070112-21$02.00/0

and this oxygen is removed by the reducing agent in a successive step. Catalysis occurs in these sequential steps. In the second model the base exchange cation is supposed to act as a template which coordinates the reacting molecules as ligands in its coordination sphere. Reaction presumably occurs by chemical transformations within the coordination sphere. In this case the sites would necessarily be within the supercages of the zeolites. For the redox model, on the other hand, it has been suggested (*1*) that the oxygen-carrying site stays within the sodalite unit, i.e., the oxygen is held as a bridge between two Fe cations located at S'_{II} and S'_{I} sites. This poses some interesting questions. How did the O atom get there in the first place? When O_2 acts as the oxidizing agent, how is it dissociated and what happens to the other half of the molecule? Similarly, if NO is the oxidizing agent, what happens to the N atom and how does it combine with another to form N_2?

Recently, Fu *et al.* (*3*) showed that the fully oxidized form of Fe–Y acted as a catalyst for N_2O decomposition. Their data supported a redox mechanism in which the oxygen-carrying site is reduced by N_2O and then reoxidized by the same reagent. It seems clear that this could not occur at a site within the cuboctahedron. Pearce *et al.* (*4*) recently used X-ray diffraction to reinvestigate the location and coordination environment of the cations in Y zeolites after a variety of pretreatment procedures. No evidence was found for the bridged oxide complex suggested earlier (*1*). Upon oxidation to Fe^{3+}, most of the iron migrated out of the hexagonal prism (Site I), in agreement with the Mössbauer spectroscopy data (*1*). Evidence of framework decomposition on repeated oxidation–reduction cycles was reported and interestingly, Fe^{2+} did not reappear at Site I upon reduction of Fe^{3+} under their experimental conditions. This is unexpected in view of the excellent reproducibility and stability exhibited by this material (*1, 2*) in oxidation–reduction cycles. Although further work is needed to make certain that the results are independent of both the preparation studied and the experimental techniques employed, it can be generally agreed that the iron can migrate from one location to another under redox conditions. Furthermore, it is likely that the cations are in dynamic motion in the zeolite lattice at the temperatures of the catalytic reactions. It is thus plausible to assume that sites for redox chemistry appear within the supercages. The present work supports this assumption.

The template model has been advanced by several workers. Most recently, Seiyama *et al.* (*5*) have shown that a satisfactory kinetic interpretation can be given in this way for the reaction of NH_3 with NO over CuY. In addition, a number of works exist (*6–13*) in which NO or CO, adsorbed on altervalent base exchange cations, has been studied near room temperature by ir and/or EPR spectroscopy. Thus, it is clear that such species can and do exist, and may play a role in catalysis. In addition, earlier work (*2*) had shown that an amount of NO equivalent to a large fraction of the oxygen-carrying capacity was adsorbed at temperatures below 470 K without release of N_2. At slightly higher temperatures the site was oxidized as N_2 was released.

The present work was undertaken to learn more about the interactions of NO with iron cations in Y zeolite. Infrared spectra of NO bound to the Fe cations have revealed the presence of several kinds of sites. Complementary Mössbauer spectroscopy data have been helpful in defining the nature of these sites and the changes which occur with time, temperature, and treatment conditions.

EXPERIMENTAL

A Nicolet model MX-1 Fourier transform spectrometer was used to obtain infrared spectra. A vacuum-tight ir cell having KBr windows was designed to fit the spectrometer, yet be attachable to a standard vacuum system with provisions for measuring gas volumes and for recirculating reactant gases. Infrared spectra were obtained at room temperature with the spectrometer operating in the absorbance mode. The resolution was maintained automatically at 2 cm^{-1} for all regions of the spectrum. Self-supporting zeolite wafers were pressed, having an areal loading of 10.3 mg/cm^2. The cell was arranged such that a zeolite wafer could be lowered into slots between the optical windows for spectroscopic examination and withdrawn upward by action of a magnet into a heated portion (self-contained furnace) for the various treatments described in the next section. Measurements of NO adsorption were made on a Cahn balance at room temperature, and temperature-programmed desorption experiments were supplemented by mass spectrometric analyses of the desorbed gases.

The Mössbauer spectrometer used in these studies of Fe–Y zeolite has been described elsewhere (*14*). An electromechanical drive, operated in a constant acceleration mode, provided the Doppler velocity modulation to a ^{57}Co source (in palladium). This generated two mirror-image Mössbauer spectra which were computer-folded into one another to generate a single Mössbauer spectrum with a flat baseline. All Mössbauer spectra were fit by a random search method with a number of quadrupole-split doublets (as described later) using the program MFIT (*15*). The velocity scale was calibrated using a sodium nitroprusside standard absorber; and, using the known isomer shift of this standard relative to metallic iron (-0.260 mm s^{-1}), all velocities are reported relative to the isomer shift of metallic iron. Approximately 0.20 g of Fe–Y zeolite was pressed into a wafer (ca. 2.5 cm in diameter), and loaded into a stainless-steel Mössbauer spectroscopy cell, the design of which has been reported elsewhere (*14*). This allowed *in situ* spectra to be obtained and catalyst treatments to be carried out at temperatures up to 700 K and pressures from ca. 10^{-3} Pa to 1 atm.

Nitric oxide was purified by a freeze–pump–thaw–distill–freeze technique. This cycle was repeated several times with a distillation between two traps, and finally the gas was passed through an isopentane slush trap (120 K) and into a storage vessel. The final liquid which was distilled was crystal clear.

RESULTS

Infrared Spectroscopy

An Fe–Y sample (containing 6.3×10^{20} Fe ions/g) which had been previously dried in air at 370 K was treated in flowing dry O_2 at temperatures which were increased in 100 K stages from 370 to 670 K and finally to 720 K; 90 min was allowed for each step. The sample was then reduced by exposure for 1 h to 200 Torr of hydrogen at 720 K in the ir cell, continuously recirculating the H_2 through the cell and then through a cold trap at 78 K to remove water. The cell was evacuated at 720 K for 1 h, cooled to room temperature, and subsequently filled with 5 Torr of NO at this temperature. Figure 1a shows the ir baseline collected prior to addition of NO to the cell, while Figs. 1b and c are the ir spectra obtained after exposure of the sample to NO for 1 min and 3 h, respectively. It can be seen that the broad band near 1870 cm^{-1} forms most quickly, and that the 1917- and 1815-cm^{-1} bands grow more slowly with time. Upon evacuation of the NO from the cell at room temperature (see Fig. 1d), the bands at 1917 and 1815 cm^{-1} decreased in intensity, a new peak appeared at 1767 cm^{-1}, and a distinct peak at 1845 cm^{-1} became resolvable in the broad band originally near 1870 cm^{-1}. When reduced Fe–Y was heated in 5 Torr of NO at 770 K and then cooled to room temperature, the spectrum of Fig. 1e resulted. Alternatively, when reduced Fe–Y was first oxidized in O_2 at 770 K, evacuated at room temperature for 15 min, and then exposed to 5 Torr of NO, the spectrum of Fig. 1f was observed.

The observation that the ir bands of Fig. 1 are different for the reduced and oxidized

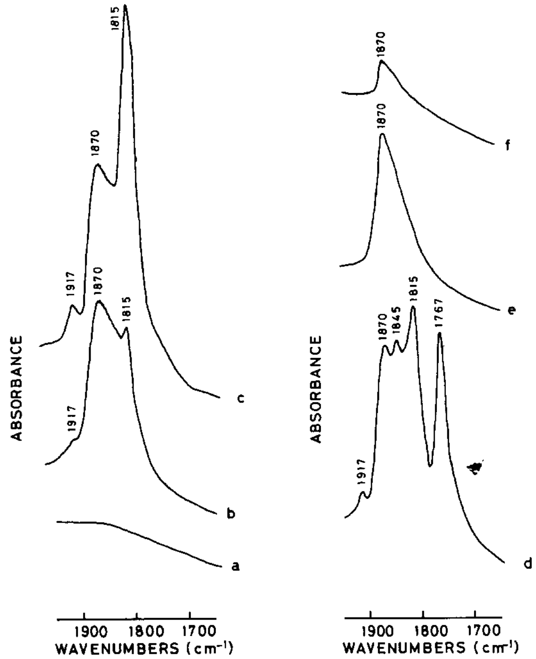

FIG. 1. Room-temperature infrared spectra of Fe-Y (Fe concn: 6.3 × 10^{20} Fe ions/g) following exposure to NO and after various thermal treatments: (a) reduced Fe-Y before addition of NO; (b) reduced Fe-Y in 5 Torr of NO for 1 min; (c) reduced Fe-Y in 5 Torr of NO for 3 h; (d) following room-temperature evacuation of sample c for 30 min; (e) after heating sample d in 5 Torr NO at 770 K for 15 min; (f) oxidized Fe-Y following evacuation at room temperature for 15 min and exposure to 5 Torr of NO.

Fe-Y samples suggests that these bands are due to iron nitrosyl complexes. This is in agreement with previous studies of NO adsorption on Y zeolite exchanged with various transition metal cations (e.g., (*8*, *9*,*16*)). Comparison of the spectral features in Figs. 1b-d also suggests that the intensities of the bands at 1917 and 1815 cm^{-1} change in parallel. This is shown more quantitatively in Fig. 2, which is a plot of the spectral intensities, I_{1917}, I_{1870}, and I_{1815} versus time of exposure to NO. The band at 1870 cm^{-1} reached its final intensity very quickly, while the intensities of the bands at 1917 and 1815 cm^{-1} both increased slowly with time. If the 1917- and 1815-cm^{-1} bands are, in fact, due to the same adsorbed species, then a plot of these data as I_{1917} versus I_{1815} should be linear. This was confirmed in Fig. 3. It is therefore suggested that the bands at 1917 and 1815 cm^{-1} are due to the symmetric and asymmetric stretching modes, respectively, from an iron dinitrosyl species. [The observation that the symmetric stretching mode has a higher frequency than the asymmetric mode is consistent with the behavior of dinitrosyl complexes (e.g., (*16*)). Furthermore, the distinction between dinitrosyl species and $(NO)_2$ dimers is not made in this paper. The term

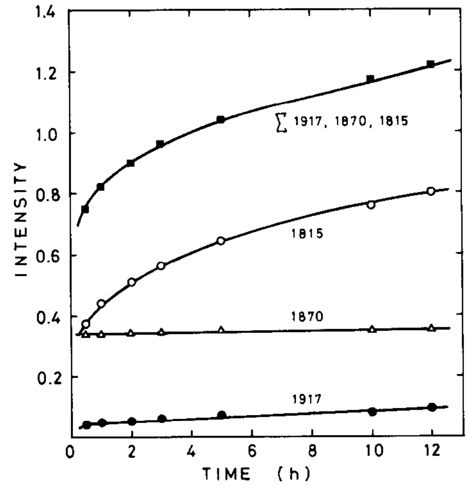

FIG. 2. Time dependence of infrared band intensities for reduced Fe-Y in 10 Torr of NO at room temperature (Fe concn: 6.3 × 10^{20} Fe ions/g).

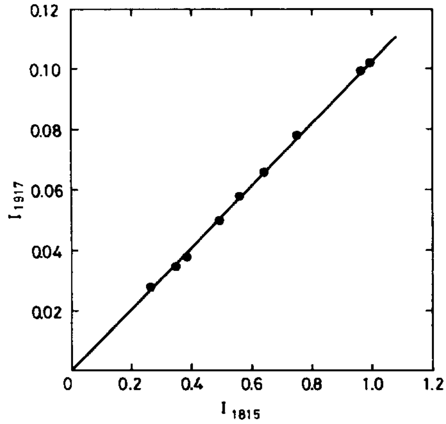

FIG. 3. Relationship between intensities of 1917- and 1815-cm^{-1} infrared bands at different coverages of NO on reduced Fe-Y at room temperature (Fe concn: 6.3 × 10^{20} Fe ions/g).

"dinitrosyl" is meant to denote two NO molecules associated with a single adsorption site.] The constant intensity ratio for these two bands implies that the angle between the two NO groups is approximately equal to 145°, and that this angle does not change with time of exposure to NO.

Studies using ^{14}NO and ^{15}NO were designed to further confirm the assignment of the bands at 1917 and 1815 cm^{-1} to an iron dinitrosyl species. Figure 4 shows the ir spectra for reduced Fe–Y zeolite obtained after long exposure to 5 Torr of ^{14}NO, ^{15}NO, and a 1 : 1 mixture of ^{14}NO and ^{15}NO. It can be seen that the band at 1815 cm^{-1} in the presence of ^{14}NO is shifted to 1778 cm^{-1} in the presence of ^{15}NO. If a mononitrosyl species were responsible for this peak, then the ir spectrum for the 1 : 1 mixture of ^{14}NO and ^{15}NO would simply be a linear (and equal) combination of these two bands at 1815 and 1778 cm^{-1}. On the other hand, if a dinitrosyl species were responsible for the band at 1815 cm^{-1} in the presence of ^{14}NO, then three bands should appear in this region of the spectrum for the 1 : 1 mixture of ^{14}NO and ^{15}NO: a band at 1815 cm^{-1} due to two ^{14}NO groups on iron, a band at 1778 cm^{-1} due to two ^{15}NO groups on iron, and an intense band between 1815 and 1778 cm^{-1} due to one ^{14}NO and one ^{15}NO group, both adsorbed on iron. Moreover, from simple statistics the relative intensities of these three bands should be 1 : 1 : 2. The observation in Fig. 4 that the spectral intensity between 1815 and 1778 cm^{-1} passes through a maximum in the 1 : 1 mixture of ^{14}NO and ^{15}NO demonstrates that the band at 1815 cm^{-1} in ^{14}NO is, in fact, due to a dinitrosyl species. Coupled with the previous observation that the intensities of the bands at 1917 and 1815 cm^{-1} change in parallel, one must also assign the band at 1917 cm^{-1} to this same dinitrosyl species.

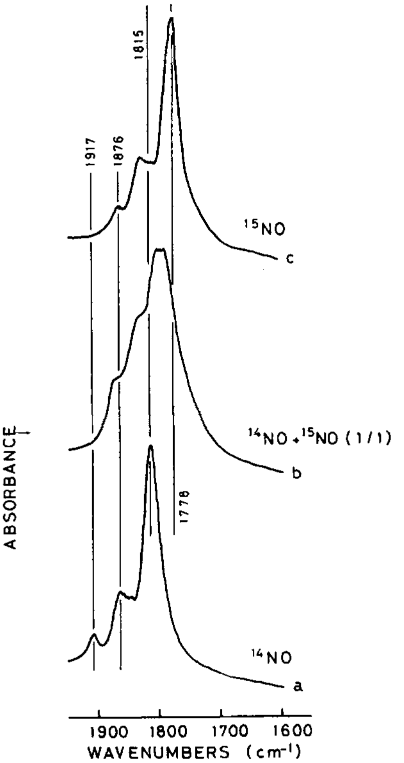

FIG. 4. ^{14}NO and ^{15}NO infrared spectra on reduced Fe–Y at room temperature (Fe concn: 6.3 × 10^{20} Fe ions/g): (a) 5 Torr of ^{14}NO for 22 h; (b) 10 Torr of ^{14}NO + ^{15}NO (1 : 1) for 24 h; (c) 5 Torr of ^{15}NO for 24 h.

To further investigate the relationships between the various NO stretching bands, infrared spectra were collected for a low-iron-loading preparation of Fe–Y (4.75 × 10^{20} Fe ions/g). The time following exposure to NO (at 5 Torr) and following evacuation of gaseous NO from the cell was varied. As shown in Fig. 5, the spectral-intensity changes were analogous to those seen in Fig. 2 for the higher-iron-loading sample with the exception that a band at 1845 cm^{-1} was resolved from the broad band near 1880 cm^{-1} (a 10-cm^{-1} shift) even in the presence of gaseous NO for the lower-iron-loading zeolite. Upon evacuation, the intensities of the bands at 1880 and 1845 cm^{-1} rapidly decreased to values slightly smaller than those in the presence of gaseous NO; the coupled bands at 1917 and 1815 cm^{-1} decreased more slowly with time to values significantly smaller than those in the presence of gaseous NO; and a band at 1767 cm^{-1} appeared and grew slowly with time of evacuation. The obser-

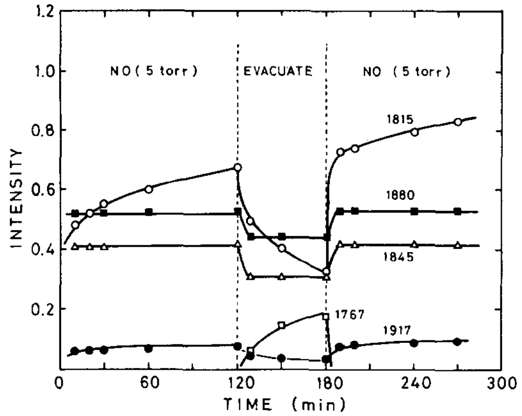

FIG. 5. Time dependence of infrared band intensities for reduced Fe-Y during exposure to 5 Torr of NO and during evacuation at room temperature (Fe concn: 4.8 × 10^{20} Fe ions/g).

vation that upon evacuation the band at 1767 cm^{-1} increased at a rate comparable to the rate of disappearance of the coupled bands at 1917 and 1815 cm^{-1}, suggested that the dinitrosyl species was being converted into a mononitrosyl species having a band at 1767 cm^{-1}. Upon evacuation this band at 1767 cm^{-1} grew to an intensity that was approximately equal to one-half of that lost by the coupled bands at 1917 and 1815 cm^{-1}. Additional evidence that the band at 1767 cm^{-1} was formed via removal of one NO group from a dinitrosyl species was that the coupled bands at 1917 and 1815 cm^{-1} were immediately reformed at the expense of the band at 1767 cm^{-1} upon readmission of gaseous NO into the ir cell (Fig. 5).

The changes in the ir spectral intensities following heat treatment under vacuum at progressively higher temperatures are shown in Fig. 6. Each point on these curves corresponds to an ir spectrum collected at room temperature following evacuation at the indicated temperature for 20 min. The intensities of the coupled bands at 1917 and 1815 cm^{-1} decreased rapidly with increasing temperature, while the intensity of the band at 1767 cm^{-1} passed through a maximum. This behavior is consistent with the conversion of 1917- and 1815-cm^{-1} dinitrosyl species into 1767-cm^{-1} mononitrosyl species at temperatures up to ca. 350 K. After vacuum treatment at higher temperatures, dinitrosyl species were no longer present, and the removal of 1767-cm^{-1} mononitrosyl species began. The intensities of the bands at 1870 and 1845 cm^{-1} showed monotonic decreases with increasing temperature, the latter band having a greater thermal stability than the former. However, unlike the coupled bands at 1917 and 1815 cm^{-1}, the changes in intensity of these bands did not parallel intensity changes of any other band. This indicates that each of these bands is due to a single species. Thus, three different mononitrosyl species can be identified on Fe-Y zeolite, and the order of decreasing thermal stability under vacuum is: 1845 cm^{-1} $\geq$ 1767 cm^{-1} $>$ 1870 cm^{-1}.

In analogous experiments, changes in the ir spectral intensities were also monitored following heat treatment in 10 Torr of NO at progressively higher temperatures. The results of these measurements are given in Fig. 7. No attempt was made to resolve the bands at 1870 and 1845 cm^{-1}, but instead a single broad band was used to describe this

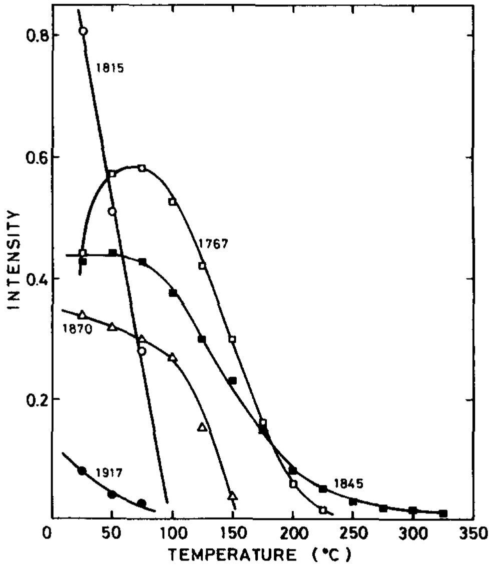

FIG. 6. Infrared band intensities at room temperature of reduced Fe-Y after exposure to NO at room temperature and evacuation at progressively higher temperatures (Fe concn: 6.3 × 10^{20} Fe ions/g).

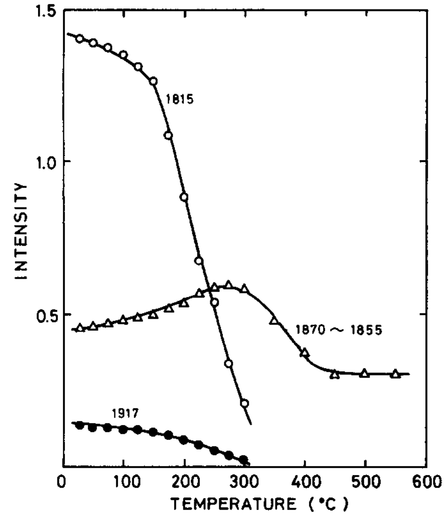

FIG. 7. Infrared band intensities at room temperature of reduced Fe–Y after exposure to 10 Torr of NO at room temperature and heating in NO to progressively higher temperatures (Fe concn: 6.3 × 10^{20} Fe ions/g).

complex portion of the ir spectrum. While the intensities of the coupled bands at 1917 and 1815 cm^{-1} decreased monotonically, the intensity of the broad band near 1860 cm^{-1} passed through a maximum with increasing temperature as the Fe^{2+}–Y was converted to Fe^{3+}–Y. In separate infrared experiments, it was shown that if NO is admitted to a calcined sample of Fe–Y zeolite that has been previously evacuated at room temperature, then a weak, broad band at approximately 1870 cm^{-1} is observed. This may correspond to the adsorption of NO on Fe^{3+}. Gravimetric measurements confirmed that the extent of NO adsorption on Fe^{3+}–Y zeolite is much smaller than that on Fe^{2+}–Y zeolite. Thus, the maximum in intensity of the band near 1860 cm^{-1} with increasing temperature may be due to two competing processes. The Fe^{2+} participating in the dinitrosyl species was apparently oxidized at temperatures below ca. 570 K, leading to a decrease in the intensity of the coupled bands at 1917 and 1815 cm^{-1}, and this was accompanied by an increase in the band intensity near 1860 cm^{-1}, arising from NO associated with Fe^{3+}. On the other hand, at temperatures above ca. 570 K, the Fe^{2+} participating in mononitrosyl species (at 1870 and 1845 cm^{-1}) was also oxidized to Fe^{3+}. This led to a decrease in the intensity of the band near 1860 cm^{-1}, because of the smaller extent of NO adsorption on oxidized Fe–Y than on the reduced form, *vide infra*. A more quantitative discussion of this oxidation of Fe^{2+} to Fe^{3+} in the presence of NO will be reserved until the results of Mössbauer spectroscopy are presented.

Another characteristic of the nitrosyl species in Fe–Y zeolite is their sensitivity to oxygen exposure at room temperature. The high-iron-loading sample (6.3 × 10^{20} Fe ions/g) was first exposed to NO, evacuated, and then exposed to 90 Torr of oxygen, all at room temperature. The resulting changes in spectral intensities are shown in Fig. 8. The bands at 1767 and 1845 cm^{-1} were immediately eliminated by exposure to oxygen, while the coupled bands at 1917 and 1815 cm^{-1} decreased more slowly with time in oxygen. The intensity of the band at 1870 cm^{-1} passed through a shallow maximum with time, suggesting the possibility that some iron was oxidized and that NO associated with Fe^{3+} gives rise to a band near 1870 cm^{-1}.

For convenience, the observed changes in infrared spectral intensity accompanying

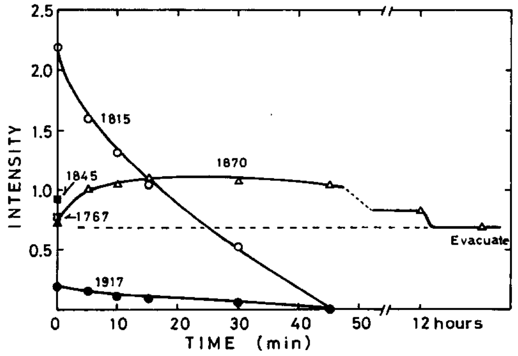

FIG. 8. Time dependence of infrared band intensities for reduced Fe–Y, which had been previously exposed to NO and evacuated at room temperature, after exposure to 90 Torr of O_2 at room temperature (Fe concn: 6.3 × 10^{20} Fe ions/g).

TABLE 1

Summary of Observed Changes in ir Spectral Intensities

Bands (cm^{-1})	Treatment					
	Exposure to NO	Heat in NO	Evacuation at room temperature	Heat under vacuum	Exposure to O_2	
1917, 1815	Gradual increase with time	Decrease with temperature; disappear at 570 K	Gradual decrease with time	Decrease with temperature; disappear at 370 K	Gradual decrease with time	A
1767	Absent	Absent	Gradual increase with time	Pass through maximum; disappear at 500 K	Rapid decrease with time	B
1845	Rapid appearance with time	Pass through maximum at 570 K; constant above 670 K	Rapid, but small decrease with time	Decrease with temperature; disappear at 520–570 K	Rapid decrease with time	C
1870	Rapid appearance with time		Rapid, but small decrease with time	Decrease with temperature; disappear at 420 K	Pass through maximum; constant at long times	D
	1	2	3	4	5	Observation

various treatments of Fe–Y zeolite are summarized in Table 1. These are given in the form of a matrix of observations, each observation denoted by a letter and a number (e.g., observation A1 indicates that the coupled bands at 1917 and 1815 cm^{-1} increase gradually with time of exposure to NO).

Gravimetric Studies

Adsorption and desorption studies of NO on Fe–Y zeolite were carried out gravimetrically, to parallel the above infrared measurements at room temperature. Figure 9 shows the time dependence of the extent of adsorption on the high-loading Fe–Y zeolite upon exposure to 5 Torr of NO. Three important observations were made: (i) on reduced Fe–Y, the initial uptake was almost doubled by a slow adsorption process; (ii) 15 to 20% of the uptake after long exposure was reversible; and (iii) the uptake on oxidized Fe–Y was significantly lower than that on the reduced material. The nature of this slow adsorption process was subsequently investigated in greater detail, as shown in Fig. 10. The recovery of NO uptake in section (c) after the evacuation at (b) was much faster than the time taken initially to go from a coverage of 0.28 mmol/g to 0.33 mmol/g. Furthermore, increasing the pressure to 24 Torr did not increase the slope of the uptake curve. The former result suggested that a slowly relaxing or irreversible structure change was induced by exposure of the zeolite to NO, and the latter indicated that this process is essentially zero order in NO (for pressures between 5 and 24 Torr).

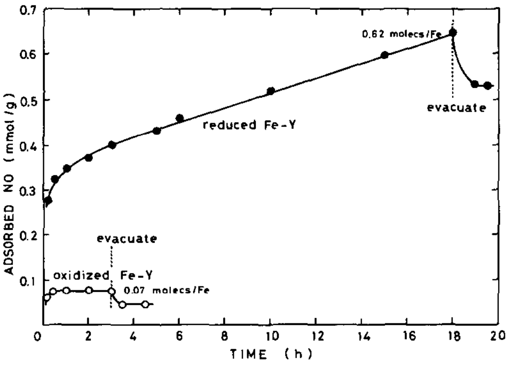

FIG. 9. Gravimetric determination of the amount of NO adsorbed on reduced and oxidized Fe–Y during exposure to 5 Torr of NO at room temperature (Fe concn: 6.3 × 10^{20} Fe ions/g).

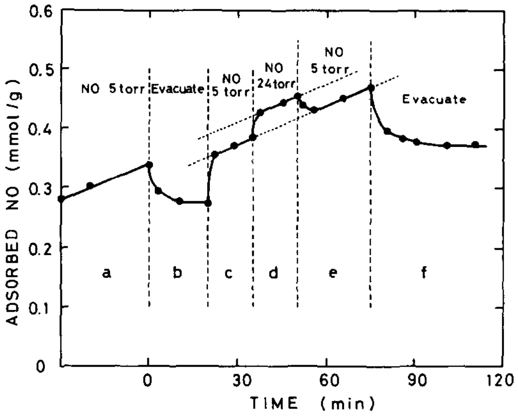

FIG. 10. Gravimetric determination of the amount of NO adsorbed on reduced Fe–Y during exposure to NO and during evacuation at room temperature. The sample was exposed to 5 Torr of NO for 3 h at Section a (Fe concn: 6.3 × 10^{20} Fe ions/g).

The thermal stability of NO on Fe–Y zeolite is shown in Fig. 11. After exposure of the sample to NO and evacuation at room temperature, temperature-programmed desorption was commenced by heating the sample at the rate of 1.6 K/min. The evolution of NO was followed mass spectroscopically while the decrease in sample weight was monitored gravimetrically. The maximum rate of NO desorption took place near

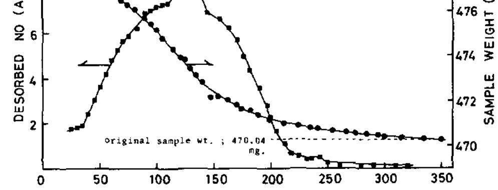

FIG. 11. Temperature-programmed desorption spectrum of NO on reduced Fe–Y (temperature increase: 1.6 K/min; Fe concn: 6.3 × 10^{20} ions/g).

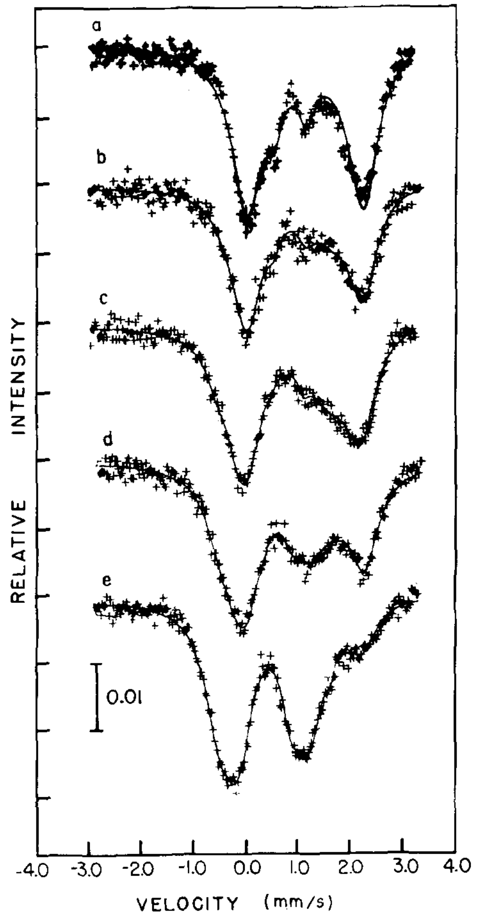

FIG. 12. Room-temperature Mössbauer spectra of reduced Fe-Y zeolite following various treatments in NO: (a) reduced Fe-Y; (b) Fe-Y in NO at 293 K; (c) Fe-Y after heating in NO at 470 K; (d) Fe-Y after heating in NO at 570 K; (e) Fe-Y after heating in NO at 670 K.

400 K, and the sample weight decreased monotonically to its original value (prior to NO exposure). This latter result indicated that oxidation of Fe-Y was not significant during temperature-programmed desorption of NO; consistent with this, N_2 and N_2O were absent in the desorption products.

Mössbauer Spectroscopy

While the interactions between NO and Fe-Y zeolite were probed by infrared spectroscopy from the NO point of view, Mössbauer spectroscopy was used to probe these interactions from the Fe point of view. After the calcined sample of Fe-Y zeolite (containing 6.3×10^{20} Fe ions/g) was loaded into the Mössbauer spectroscopy cell fitted with Teflon-coated Kapton windows (Dupont) (*14*), it was reduced in flowing hydrogen for 6 h at 670 K, cooled to room temperature, and then evacuated at this temperature. The Mössbauer spectrum subsequently collected is shown in Fig. 12a. This spectrum can be fit by two Fe^{2+} quadrupole-split doublets (*1*). The negative-most peaks of each doublet overlap, while the positive-most peaks are resolved distinctly. The doublet having the smaller isomer shift and quadrupole splitting will be denoted as the "inner doublet," and it has been attributed to Fe^{2+} in the low-coordination S'_{I}, S'_{II}, or S_{II} sites (*1*). The doublet having the larger isomer shift and quadrupole splitting will be denoted as the "outer doublet," and it has been attributed to Fe^{2+} in the high-coordination S_{I} site (*1*). The reduced and evacuated Fe-Y zeolite was then exposed to ca. 100 Torr of NO at room temperature, and the spectrum of Fig. 12b was collected. Subsequently, the sample was heated in the presence of NO to 470 K for 0.5 h and cooled to room temperature, at which point a Mössbauer spectrum was collected. This was followed by analogous treatments in NO at 570 and 670 K. The corresponding spectra are shown in Figs. 12c–e. These Mössbauer spectroscopy experiments parallel the ir experiments summarized in Fig. 7.

Computer fitting of overlapping components in a Mössbauer spectrum must be performed by constraining the various peaks to have physically meaningful values. In the present study, this was done by using a small number of doublets with fixed Mössbauer parameters (i.e., isomer shift and quadrupole splitting) to fit all of the Mössbauer spectra for a given Fe-Y sample following various treatments. In this way, the Mössbauer parameters of these doublets were determined by considering together all of the Mössbauer spectra for that sample, instead of fitting each spectrum independently. This makes it possible to analyze a given spectrum in terms of a larger number of doublets than would be justifiable if that spectrum were fit without regard to related spectra of the same sample. Accordingly, the five spectra of Fig. 12 were first fit by varying the relative intensities of five different quadrupole-split doublets. Physically, these doublets correspond to (i) the Fe^{2+} inner doublet, (ii) the Fe^{2+} outer doublet, (iii) NO associated with Fe^{2+}, and (iv), (v) two Fe^{3+} doublets. Two different Fe^{3+} doublets were used in these fits due to the inability of a single Fe^{3+} doublet to adequately fit the spectrum taken following treatment in NO at 670 K (Fig. 12e). These two Fe^{3+} species have similar isomer shifts but differ in their quadrupole splittings. (The Fe^{3+} doublet with larger quadrupole splitting represents an iron cation in a site of greater deviation from cubic symmetry.) The isomer shift and quadrupole splitting of each doublet were constrained to be the same in each of the five spectra, i.e., only the dip and width of each doublet were allowed to vary between different spectra. It should also be noted that the pair of peaks comprising a given doublet were constrained to have the same dip and width.

It may be questioned why only one Mössbauer spectral doublet was assigned to NO associated with Fe^{2+}, in view of the fact that three different nitrosyl species were observed by ir in the presence of NO: mononitrosyls at 1845 and 1870 cm^{-1} and a dinitrosyl species. First, the use of one doublet due to nitrosyl species gave rise to good fits of the Mössbauer spectra, and the inclusion of additional doublets was not warranted. Furthermore, it will be discussed later in this paper that Fe^{2+} cations associated with dinitrosyl species have a low recoil-free fraction, and are not observed in the spectra of Fig. 12. Thus, the Mössbauer spectral doublet assigned to Fe^{2+} cations associated with NO is related to the mononitrosyl species observed in the ir at 1845 and 1870 cm^{-1}.

The results of the above fitting procedure are summarized in Table 2. Therein are shown the isomer shifts (*IS*), quadrupole splittings (*QS*), peak widths (Γ, full width at half-maximum dip), and spectral areas for each of these five doublets in the five spectra of Fig. 12. The isomer shifts and quadrupole splittings of the Fe^{2+} inner doublet, Fe^{2+} outer doublet, and Fe^{3+} doublets all agree well with published values for these species in Y zeolites (*1*). Published Mössbauer data for NO associated with Fe^{2+} in Y zeolites, however, are not available for comparison with the present study. To further test the validity of the present fitting procedure, the parameters from these constrained fits were used as the input values in unconstrained fits of the spectra. During this procedure, the pairs of peaks comprising the five doublets were still constrained to have equal dips and widths. The results of the constrained and unconstrained fits were very similar, with isomer shifts varying by less than 0.02 mm s^{-1} and quadrupole splittings varying by less than 0.08 mm s^{-1}. This suggests that the spectra of Fig. 12 can indeed be adequately fit by simply varying the relative intensities of five constrained doublets.

The changes in spectral areas accompanying the different thermal treatments in NO are shown in Fig. 13. The amount of iron not associated with NO (i.e., giving rise to the inner and outer doublets) decreased upon exposure of Fe–Y zeolite to NO at room temperature. This was accompanied by the appearance of the doublet associated with NO adsorbed on Fe^{2+}. The presence of Fe^{3+} was not detected until the temperature was raised to 470 K. At this temperature, the amount of inner doublet was insignificant and only a trace of Fe^{3+} was present. As the temperature was raised above 470 K, the spectral areas of both Fe^{3+} doublets increased at the expense of the outer doublet and the doublet associated with NO on Fe^{2+}.

TABLE 2

Mössbauer Parameters for Fe–Y Spectra in Fig. 12

Spectral lines	Parameter	Reduced Fe–Y	Fe–Y exposed to NO at 298 K	Fe–Y heated in NO at 470 K	Fe–Y heated in NO at 570 K	Fe–Y heated in NO at 670 K
Outer doublet	*IS*	1.14	1.14	1.14	1.14	1.14
	QS	2.24	2.24	2.24	2.24	2.24
	Γ	0.69	0.69	0.81	0.70	0.67
	A	4.86	3.34	3.56	2.75	1.25
Inner doublet	*IS*	0.87	0.87	0.87	0.87	
	QS	0.63	0.63	0.63	0.63	
	Γ	0.43	0.43	0.22	5.8	
	A	0.93	0.55	0.08	0.01	
NO – Fe^+	*IS*		0.79	0.79	0.79	0.79
	QS		1.70	1.70	1.70	1.70
	Γ		0.80	0.88	0.79	0.26
	A		1.10	1.85	0.92	0.26
$Fe^{3+}_{(A)}$	*IS*			0.34	0.34	0.34
	QS			1.71	1.71	1.71
	Γ			0.39	0.71	0.69
	A			0.23	1.78	3.71
$Fe^{3+}_{(B)}$	*IS*			0.32	0.32	0.32
	QS			1.08	1.08	1.08
	Γ			0.22	0.41	0.40
	A			0.02	0.54	1.16
	Total area (% × mm/s)	5.79	4.99	5.74	6.00	6.38

Note. IS = Isomer shift relative to Fe^0 (mm/s). *QS* = Quadrupole splitting (mm/s). Γ = Linewidth, same for both peaks (mm/s). *A* = Spectral area (% × mm/s).

The effects of thermal treatments under vacuum, following NO adsorption at 298 K, were also investigated using Mössbauer spectroscopy to parallel the ir studies summarized in Fig. 6. For this series of experiments, the Teflon-coated Kapton windows of the Mössbauer spectroscopy cell were replaced by beryllium windows to avoid complications from the possible diffusion of H_2O and/or O_2 (from the air into the cell) through the Kapton windows during vacuum treatments. Details of the beryllium windows and the iron impurities found in them are given by Shen *et al.* (*17*). The spectral component arising from this iron impurity was fit with a quadrupole-split doublet, the isomer shift and quadrupole splitting of which were determined by collecting Mössbauer spectra of the cell without a zeolite sample. In addition, the spectral area of this doublet was constrained to be the calibrated value in computer fits of all subsequent Mössbauer spectra. Figures 14a and b depict the room-temperature spectra for a hydrogen-reduced Fe–Y zeolite (containing 6.0×10^{20} Fe ions/g) and for this sample after exposure to ca. 100 Torr of NO, respectively. The spectral features of Figs. 14a and b are nearly identical to those of Figs. 12a and b. A Mössbauer spectrum was subsequently collected (Fig. 14c) at room temperature after reducing the vapor pressure of NO to ca. 0.1 Torr by immersing a Pyrex appendage, which was attached to the cell, into liquid nitrogen. The desorption of NO from the sample was then fur-

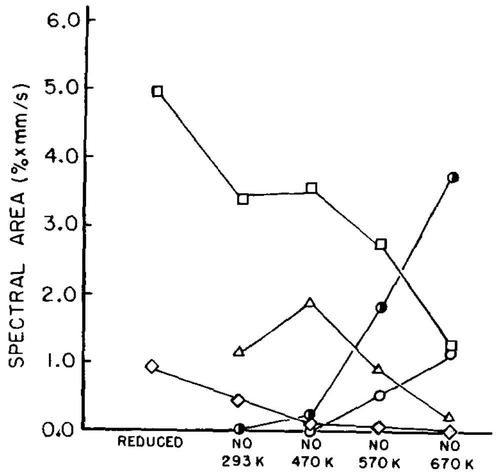

FIG. 13. Spectral-area changes for the Mössbauer spectra of Fig. 12: (□) outer doublet of reduced Fe–Y; (◇) inner doublet of reduced Fe–Y; (△) doublet due to NO associated with Fe^{2+}; (○) Fe^{3+} doublet (small quadrupole splitting); (◑) Fe^{3+} doublet (large quadrupole splitting).

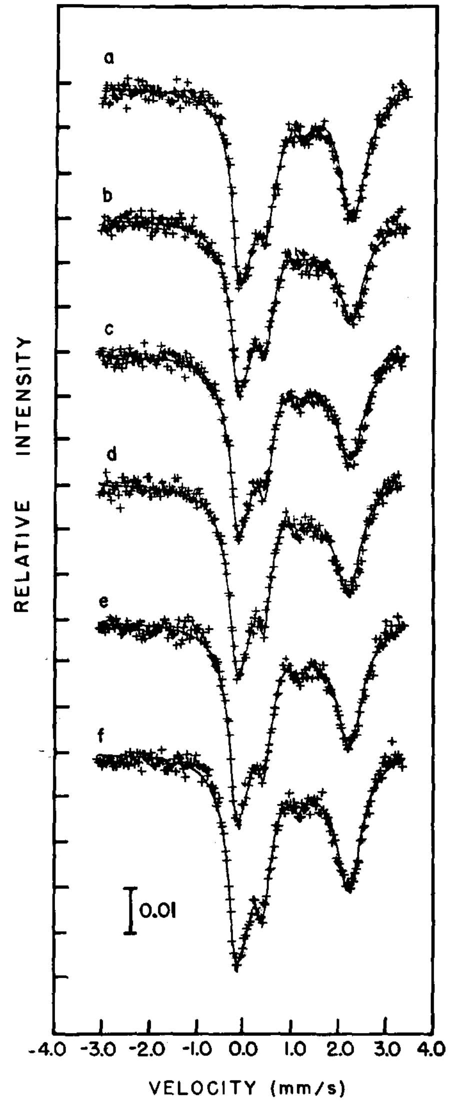

FIG. 14. Room-temperature Mössbauer spectra of reduced Fe–Y zeolite following exposure to NO and evacuation at various temperatures: (a) reduced Fe–Y; (b) Fe–Y in NO at 293 K; (c) Fe–Y in 0.1 Torr NO at 293 K; (d) Fe–Y following evacuation of NO at 293 K; (e) Fe–Y following evacuation of NO at 400 K; (f) Fe–Y following evacuation of NO at 570 K.

ther studied by evacuating the cell at room temperature (to ca. 10^{-6} Torr) and successively heating under vacuum for 0.5 h at 400 and 570 K. After each of these three evacuations, a room-temperature Mössbauer spectrum was collected, and these are shown in Figs. 14d–f.

The five quadrupole-split doublets used to fit the Mössbauer spectra of Fig. 12 were used as the bases for constrained computer fits of the spectra in Fig. 14, with the addition of the doublet due to iron impurities in the beryllium windows of the cell. Table 3 summarizes the results of this procedure for each of the spectra of Fig. 14. The spectral-area changes that occurred as a result of the adsorption of NO and the subsequent evacuation treatments are shown in Fig. 15. Adsorption of NO caused a decrease in the areas associated with the inner and outer doublets and the appearance of the doublet associated with NO on Fe^{2+}. (This is analogous to the spectral-area changes of Fig. 13 accompanying exposure of Fe–Y zeolite to NO at room temperature.) Decreasing the NO pressure to ca. 0.1 Torr or evacuation at room temperature caused no change in the spectral areas of the inner doublet or the doublet associated with NO adsorbed on Fe^{2+}; however, the spectral area of the outer doublet increased in each instance. Heating under vacuum at 400 and 570 K caused further increases in the spectral area of the outer doublet. The spectral area of

TABLE 3

Mössbauer Parameters for Fe–Y Spectra in Fig. 14

Spectral lines	Parameter	Reduced Fe–Y	Fe–Y exposed to NO at 293 K	Fe–Y at 293 K in 0.1 Torr NO	Fe–Y evacuated at 293 K	Fe–Y evacuated at 400 K	Fe–Y evacuated at 570 K
Outer	Γ	0.57	0.63	0.67	0.69	0.65	0.65
doublet	A	5.61	3.81	4.42	4.57	5.31	5.76
Inner	Γ	0.65	0.57	0.28	0.38	0.41	0.42
doublet	A	0.87	0.39	0.32	0.36	0.80	0.87
NO–Fe^{2+}	Γ		1.03	0.86	1.01	0.48	0.40
	A		1.12	1.11	1.13	0.46	0.37

the inner doublet increased upon evacuation at 400 K, followed by a slight increase in area upon evacuation at 570 K, and these area increases of the inner doublet were paralleled by corresponding decreases in the spectral area of the doublet associated with NO adsorbed on Fe^{2+}. No Fe^{3+} was present in the spectra of Fig. 14, consistent with the gravimetric desorption experiments which indicated no oxidation of Fe^{2+}–Y zeolite during desorption of NO under vacuum.

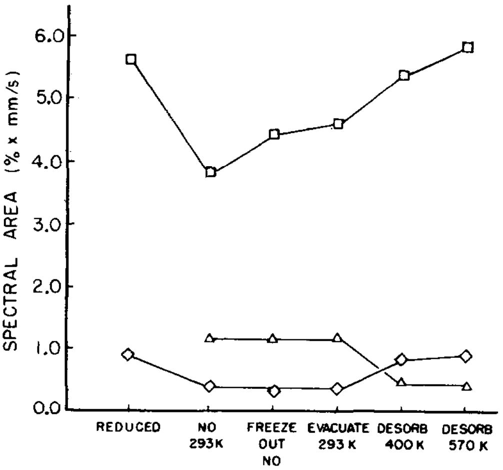

FIG. 15. Spectral-area changes for the Mössbauer spectra of Fig. 14: (□) outer doublet of reduced Fe–Y; (◇) inner doublet of reduced Fe–Y; (△) doublet due to NO associated with Fe^{2+}.

DISCUSSION

General Features of NO Interaction with Fe^{2+}–Y Zeolite

A general interpretation of the infrared spectral behavior outlined above can be given in terms of the accessibility of the iron cations to nitric oxide. For steric reasons, it is proposed that the coupled bands at 1917 and 1815 cm^{-1} are due to two NO groups adsorbed on a "highly accessible" iron cation. Then, since the band at 1767 cm^{-1} is formed from this dinitrosyl species upon evacuation, it follows that this low-frequency band is due to a single NO group on the highly accessible iron. With this interpretation it is possible to explain several of the spectral observations shown in Table 1. Due to the coordinative unsaturation of this highly accessible iron (in the absence of NO), NO should be strongly bound to this iron (observation B4) and this iron may be very susceptible to oxygen addition (observation B5).

In contrast, it is proposed that the band at 1870 cm^{-1} is due to an NO group adsorbed on a "sterically hindered" iron cation. It may be argued that as the NO stretching frequency of a mononitrosyl species increases, the Fe–N–O group becomes more linear (*18*). Thus, while the NO on highly accessible iron is free to assume a partially bent configuration (leading to the band at

1767 cm^{-1}), the NO group on sterically hindered iron is forced to assume a more linear configuration (leading to the band at 1870 cm^{-1}) by the oxygen anions in the coordination shell of iron. Support for this statement is again found in Table 1. Because the coordinative unsaturation of sterically hindered iron is less than that of highly accessible iron, NO is not bound as strongly to the former as to the latter (observations BD4) and this iron may not be as susceptible to oxygen addition as is the latter iron (observation D5). In addition, the sterically hindered iron is not as susceptible to oxidation by NO as is the dinitrosyl species associated with highly accessible iron (observations A2, CD2).

Following the above argument that the NO stretching frequency correlates with the steric environment of iron, it is proposed that the band at 1845 cm^{-1} is due to an NO group on an iron cation of "intermediate accessibility." With reference to Table 1, this would explain why, on the one hand, NO is strongly bound (observation C4) and this iron is very susceptible to oxygen addition (observation C5), while on the other, it is apparently less susceptible to oxidation by NO than is the dinitrosyl species on highly accessible iron (observations A2, CD2).

The rate of appearance of the various infrared bands upon exposure of Fe–Y zeolite to NO is consistent with the above interpretation. The bands at 1870 and 1845 cm^{-1} appear very rapidly with time of exposure to NO, suggesting that sterically hindered iron and iron cations of intermediate accessibility are already present prior to exposure to NO. The coupled bands at 1917 and 1815 cm^{-1}, however, grow slowly with time, and this process appears to be zero order with respect to the NO pressure (from 5 to 24 Torr). This suggests that the highly accessible iron associated with the dinitrosyl species is formed by migration of iron cations from other sites in the zeolite which are energetically more favorable in the absence of NO.

If the migration of iron to form dinitrosyl species involved the intermediate formation of mononitrosyl species, then the intensity of at least one of the infrared bands associated with mononitrosyl species (i.e., at 1870, 1845, or 1767 cm^{-1}) would pass through a maximum with time of exposure to NO. Instead, Figs. 2 and 5 show that the bands at 1870 and 1845 cm^{-1} immediately reach constant intensities with time, and the band at 1767 cm^{-1} is not observed in the presence of NO. This suggests that the iron associated with the dinitrosyl species migrates from a site where it cannot form either a mononitrosyl or a dinitrosyl complex to a location of high accessibility. In addition, during this migration the iron does not pass through those sites at which the 1870- and 1845-cm^{-1} mononitrosyl species are formed.

The gravimetric measurements of Fig. 9 indicate that on the average, approximately 0.62 molecules of NO are associated with each iron cation after long exposure to NO at room temperature. The Mössbauer spectrum of Fig. 12a shows that prior to exposure of Fe–Y zeolite to NO, 84 and 16% of the Fe^{2+} is present as outer-doublet and inner-doublet species, respectively. Then, upon long exposure to NO at room temperature, the absolute spectral areas of the outer and inner doublets decrease to 65 and 50% of their original values (see Table 2). If it is assumed that the outer and inner doublets have equal recoil-free fractions, then it can be calculated that after exposure to NO, 29 and 8% of the Fe^{2+} in Fe–Y zeolite is present as NO associated with iron cations which were originally contributing to the outer and inner doublets, respectively. Accordingly, if the dinitrosyl and mononitrosyl species are associated with iron cations from the inner and outer doublets, respectively, then the average NO-to-Fe^{2+} stoichiometry would be 0.45. On the other hand, an average NO-to-Fe^{2+} stoichiometry of 0.66 is calculated assuming that the dinitrosyl and mononitrosyl species are associated with iron cations from the outer and inner doublets, respectively. The gravimetric data support the latter interpretation.

It has been proposed (*1*) that the outer doublet is due to highly coordinated iron cations which are inaccessible to gaseous molecules, while the inner doublet is due to iron cations of lower coordination which are more accessible. Thus, the iron cations originally contributing to the outer doublet must migrate to other sites if they are to form dinitrosyl species with NO, while in contrast, the iron cations contributing to the inner doublet may already be accessible to gaseous NO. This behavior would be consistent with the observation that dinitrosyl species are formed slowly with time of exposure to NO, while the mononitrosyl species are formed much more rapidly. It is therefore suggested that the migration of iron to form dinitrosyl species is due to the movement of iron cations from outer-doublet sites to sites of high accessibility, and that the formation of mononitrosyl species (at 1870 and 1845 cm^{-1}) is due to adsorption of NO on inner-doublet sites which are already accessible prior to introduciton of NO. In addition, during this migration of cations from outer-doublet sites to highly accessible sites in the presence of NO, the iron does not pass through the inner-doublet sites.

As noted previously, infrared spectroscopy is able to distinguish the presence of three different mononitrosyl and dinitrosyl species, while the results of Mössbauer spectroscopy differentiate only one new doublet upon exposure to NO. However, Figs. 13 and 15 show appreciable spectral-area losses of both the inner and outer doublets following the adsorption of NO. The close parallel between the spectral-area changes of the inner doublet with the corresponding changes in the area of the doublet associated with NO adsorbed on Fe^{2+}, as seen in Fig. 15, suggests that this latter doublet can be assigned to mononitrosyl species formed as the result of NO adsorption on inner-doublet Fe^{2+}. This assignment implies that the dinitrosyl species present at room temperature, due to the interaction of NO with outer-doublet Fe^{2+}, is not observable by Mössbauer spectroscopy. This type of behavior has been observed previously (*1*) for the interactions of $\mathrm{H_2O}$, $\mathrm{NH_3}$, and other adsorbates with Fe^{2+} in Y zeolite. It has been attributed to a weakening of the bonding of the iron cations to the zeolite framework due to the interaction of these cations with adsorbed molecules. This leads to a reduction in the recoil-free fraction of iron and a corresponding decrease in Mössbauer spectral area. In fact, it can be seen in Tables 2 and 3 that the total Mössbauer spectral area decreases upon exposure of Fe–Y zeolite to NO at room temperature, and that it increases following subsequent heat treatment in either NO or under vacuum. Accordingly, exposure of Fe–Y zeolite to NO at room temperature leads to the formation of dinitrosyl species, while heat treatment in either NO or under vacuum leads to the destruction of these species (as seen in Figs. 6 and 7). It is thus suggested that NO adsorbed on inner-doublet Fe^{2+} leads to mononitrosyl species having an observable Mössbauer spectrum, while two NO molecules adsorbed on Fe^{2+} originating from the outer doublet produce a dinitrosyl species with a very small recoil-free fraction.

Figure 5 shows that, upon evacuation at room temperature, dinitrosyl species are converted into mononitrosyl species at 1767 cm^{-1}. Figure 15 shows that the Mössbauer spectral area of the outer doublet increases during this treatment. On the basis of Mössbauer spectroscopy alone, this spectral-area increase could be explained by the diffusion of Fe^{2+} cations from sites of accessibility (where dinitrosyl formation occurs) to those sites of high coordination which were originally populated by Fe^{2+} in the absence of NO. In view of the infrared spectroscopy results, however, this diffusion process does not take place upon evacuation at room temperature, since reexposure to NO quickly restores the intensities of the coupled, dinitrosyl bands. If the highly accessible iron cations had, in fact, diffused to sites of high coordination upon room-temperature evacuation, then these cations would have to diffuse back to sites of high accessibility upon reexposure to NO and the resulting dinitrosyl bands would have grown slowly with time. It is thus concluded that the increase in Mössbauer spectral area upon evacuation of NO at room temperature is due to the formation of the mononitrosyl species at 1767 cm^{-1}, and that the iron associated with this species gives rise to a Mössbauer spectrum which is similar to that of the highly coordinated Fe^{2+} of the outer doublet. To test the validity of this conclusion the area of the outer doublet in the Mössbauer spectrum collected after evacuation of the NO at room temperature was constrained to be equal to the area of this doublet in the Mössbauer spectrum collected in the presence of NO. The computer was then allowed to determine the Mössbauer parameters of the doublet which was formed upon evacuation of the NO at room temperature. The parameters of this doublet (IS = 1.18 mm s^{-1} and QS = 2.11 mm s^{-1}) were very similar to those of the outer doublet. Therefore, the iron cations of the 1767-cm^{-1} mononitrosyl species are in a highly coordinated environment, similar to that of Fe^{2+} cations of the outer doublet. The results of computer fitting shown in Fig. 15 must accordingly be interpreted in terms of two highly coordinated iron species: Fe^{2+} cations associated with 1767-cm^{-1} mononitrosyl species and outer-doublet Fe^{2+} cations which are not associated with adsorbed NO. Figure 15 shows that the area of the outer doublet increases further upon evacuation at 400 and 570 K. This is due to two processes. At the lower evacuation temperature (400 K), the increase in area of the outer doublet stems chiefly from the conversion of dinitrosyl species into 1767-cm^{-1} mononitrosyl species (as seen in the infrared band intensities of Fig. 6). At the higher evacuation temperature (570 K), the increase in area of the outer doublet is due to the desorption of NO associated with mononitrosyl species and the generation of Fe^{2+} cations in sites of high coordination (without adsorbed NO).

It should be noted that Jermyn *et al.* (*8*) probed the interactions of NO with Fe–Y zeolite using infrared and EPR spectroscopies. Their reported infrared spectra show bands at 1930, 1890, 1850, 1822, and 1778 cm^{-1}, similar to the results of the present study. In addition, these authors also observed the growth of the band at 1778 cm^{-1} upon evacuation of the sample at room temperature, and they stated that this band was formed at the expense of the band at 1822 cm^{-1}. Accordingly, they mentioned the possibility that dinitrosyl complexes may exist in Fe–Y prior to evacuation. The results of the present study firmly establish this earlier postulate and, furthermore, demonstrate that the formation of these dinitrosyl complexes involves migration of Fe^{2+} cations in the zeolite structure. By comparison of ir and EPR spectra, Jermyn *et al.* also suggested that the ir band at 1890 cm^{-1} was due to a high-spin nitrosyl complex, while the ir band at 1778 cm^{-1} was due to a low-spin nitrosyl complex. Both of these complexes were considered formally to contain Fe(I). As discussed elsewhere (*1*), the Fe^{2+} cations of the outer doublet must be in a high spin state, while the spin state of the inner-doublet Fe^{2+} cations is uncertain. There are little data to support assignment of Fe(I) states, but the isomer shift of the low spin configuration is expected to be low ($\simeq$0.3 mm s^{-1}), while that of the high spin state is expected to be high ($\simeq$2 mm s^{-1}) (*19*). Thus the high isomer shift (i.e., outer-doublet character) of the iron mononitrosyl species with the ir band at 1767 cm^{-1} appears to be in conflict with the low spin assignment of the EPR data. The origin of this discrepancy between the present study and the work of Jermyn *et al.* is not currently understood. Resolution of this problem may require a more precise picture of the electron distribution in the $[FeNO]^{2+}$ complex.

Location of Iron Cations Associated with Nitrosyl Species in Fe–Y Zeolite

Steric considerations require that the iron dinitrosyl species be located in the supercages. From the gradual growth of the coupled infrared bands at 1917 and 1815 cm^{-1}, it was argued above that the highly accessible iron associated with the dinitrosyl species in the presence of the gaseous NO migrates from sites that are inaccessible to NO. These inaccessible sites are responsible for the outer doublet in the Mössbauer spectrum of reduced Fe–Y zeolite, and this doublet has previously been attributed to iron in Site I (i.e., inside the hexagonal prisms). It is tempting to speculate that the above migration involves the movement of iron from Site I to Site III′, the latter being in the supercages on four-member oxygen rings. As depicted elsewhere (*20*), this site is made up of a rectangle comprised of two O_1 and two O_4 oxygens at the corners and is centered over an underlying O_3. Thus, the Fe^{2+} need only slide from the center of the hexagonal prism into a ready-made hole of appropriate size which opens into the supercage. The attraction of this model is that the iron can migrate from an inaccessible site to a highly accessible one, without passing through sites of intermediate accessibility at which mononitrosyl species could form. It should be noted that the NO does not necessarily induce the migration of iron, since the iron is originally located in sites which are not accessible to NO. Instead, the iron cations could be in dynamic motion and reach the sites in the absence of NO, and the role of NO may be to trap the iron when it becomes accessible (e.g., at Site III′) by forming stable nitrosyl complexes with it (i.e., either a dinitrosyl species in the presence of gaseous NO or a mononitrosyl species at 1767 cm^{-1} on evacuation). The symmetry of Site III′ is such that the formation of the 1767-cm^{-1} mononitrosyl species results in a nearly octahedral coordination for the iron cation. This species gives rise to a Mössbauer spectrum which is similar to that of the outer-doublet Fe^{2+} cations (the latter also being present in nearly octahedral coordination).

It was argued from the rapid appearance of mononitrosyl bands in the infrared, that the iron associated with these complexes must be at sites which are accessible to NO even before the sample is exposed to NO. These iron cations are associated with the inner doublet in the Mössbauer spectrum of reduced Fe–Y zeolite, and this doublet has previously been attributed to iron at Sites I′, II′, and/or II. All three of these sites are associated with the hexagonal six-member rings of the sodalite cages. Site I′ is in the sodalite cage, on the six-member rings that join this cage to the hexagonal prisms. Since NO does not readily enter the sodalite cage, this site is not accessible to NO. Site II′ is also in the sodalite cage, on the six-member rings that join this cage to the supercages. This site is, therefore, more accessible to NO than is Site I′. It is conceivable that NO can reach Site II′ by adsorbing through the hexagonal window between the sodalite cage and the supercage. Site II is in the supercages, on the six-member rings that join this cage to the sodalite cages. For this reason, it is readily accessible to NO. One may now postulate that the sterically hindered iron associated with the mononitrosyl band at 1870 cm^{-1} is present at Site II′, and the iron of intermediate accessibility associated with the mononitrosyl band at 1845 cm^{-1} is present at Site II. The reason why these cations do not apparently migrate from one to the other or to sites of higher accessibility (as do the cations at Site I) may be related to the presence of OH^- or O^{2-} ligands associated with them within the sodalite cages. Ferrous cations at Site I do not have such extra ligands.

It can be seen in Fig. 13 that not all of the iron contributing to either the inner or outer doublets is accessible to NO at room temperature. In particular, iron at sites responsible for the inner doublet persists in the presence of NO at temperatures up to ca. 470 K. This may be due to iron at Site I′, which would not be readily accessible to NO at low temperatures, but would contribute to the inner doublet. Iron at sites responsible for the outer doublet can be observed at temperatures up to ca. 670 K. This may indicate that while some of the iron cations at Site I migrated to Site III′ in the presence of NO at room temperature, another portion did not, e.g., an equilibrium was established.

Since Sites II and III′ are both located in the supercages it may be questioned why the former sites apparently give rise to mononitrosyl species at 1845 cm^{-1}, while the latter sites apparently are responsible for mononitrosyl species at 1767 cm^{-1}. It has been proposed by Enemark and Feltham (*18*) that for square-planar Fe^{2+} complexes, NO coordinates in a partially bent configuration and has a low NO stretching frequency, while trigonal bipyramidal complexes of Fe^{2+} with NO show a more linear Fe–N–O configuration and have a higher NO stretching frequency. Since the iron in Site III′ is coordinated to five oxygen anions, four of which are in a square configuration, and the iron in Site II is coordinated to only three oxygen anions in a triangular configuration, the propensity of the former iron to form a mononitrosyl species with a low NO stretching frequency may be thereby explained. Also, the iron at Site III′ is apparently better able to form a dinitrosyl species in the presence of gaseous NO than is the iron at Site II for reasons which are not understood, but may be steric in nature.

Effects of Oxygen Exposure and Thermal Treatments in NO

It was noted earlier (see Fig. 8) that after exposure of Fe–Y to NO followed by evacuation at room temperature, the bands at 1845 and 1767 cm^{-1} were rapidly eliminated by addition of oxygen. This is consistent with the interpretation that the iron associated with these mononitrosyl species is located in the supercages (at Sites II and III′). The dinitrosyl bands at 1917 and 1815 cm^{-1} decreased more slowly with time upon addition of oxygen at room temperature. Evidently, the presence of two NO groups decreased the accessibility of Fe^{2+} to oxygen, since both the dinitrosyl species and the mononitrosyl species at 1767 cm^{-1} are associated with Fe^{2+} at the same site. The mononitrosyl species at 1870 cm^{-1} is apparently even less accessible to oxygen, as the intensity of this band decreased only slowly with time after exposure to oxygen. The assignment of this band to NO on iron at Site II′ in the sodalite cages is consistent with the slow reaction of this iron with oxygen at room temperature.

After exposure to NO at room temperature, heating Fe–Y to ca. 470 K in the presence of NO leads to an increase in the intensity of the ir band near 1860 cm^{-1} (see Fig. 7). Correspondingly, the Mössbauer spectral area of the doublet associated with NO adsorbed on Fe^{2+} increased at the expense of the inner-doublet area, as shown in Fig. 13. This is consistent with the assignment of the former doublet to the 1845- and 1870-cm^{-1} mononitrosyl species associated with iron cations of the inner doublet (at Sites II and II′, respectively). Both the Mössbauer spectral area of the outer doublet and the intensity of the dinitrosyl bands in the infrared remained nearly constant for heat treatments in NO at temperatures up to ca. 470 K (see Figs. 13 and 7, respectively). This supports the previous contention that dinitrosyl species are formed from iron cations which originate as outer-double Fe^{2+}. Upon heating to 570 K, Fig. 7 shows that the dinitrosyl species have been eliminated, and the band near 1860 cm^{-1} increases in intensity. Correspondingly a significant amount of Fe^{3+} was produced, as shown by Mössbauer spectroscopy (see Fig. 13). The oxidation of Fe^{2+} to Fe^{3+} by NO at this temperature is expected from the recent work of Fu *et al.* (*2*). Hence, the Fe^{2+} associated with the dinitrosyl species was oxidized at temperatures between ca. 420 and 570 K, and the resulting Fe^{3+} produced the mononitrosyl species near 1860 cm^{-1}. Finally, after heating to 670 K, nearly all of the Fe^{2+} was converted to Fe^{3+} (see Fig. 13), and the intensity of the infrared band near 1860 cm^{-1} decreased due to oxidation of the Fe^{2+} associated with the mononitrosyl species at 1870 cm^{-1}. It is interesting to note that following heat treatment in NO at 770 K, the intensity of the band near 1860 cm^{-1} was significantly greater than the intensity of this band following exposure of NO to a Fe–Y sample which had been previously oxidized in O_2 at 770 K (and evacuated at room temperature for 15 min). This implies that the Fe^{3+} formed during heat treatment in NO is more accessible to NO than Fe^{3+} formed during heat treatment in O_2. As discussed previously, the Mössbauer spectra of Fig. 12 were fit using two Fe^{3+} doublets corresponding to Fe^{3+} in sites of different deviations from cubic symmetry. Oxygen bridges between Fe^{3+} in Sites I′ and II′ have been used to interpret the Mössbauer spectrum of Fe–Y following oxygen treatment, and these bridges may also be formed upon oxidation by NO. In this configuration both ferric cations are surrounded by four oxygen anions. A second environment for Fe^{3+}, however, may result following the oxidation of Fe^{2+} in Site III′ by NO. An O^{2-} ion may cap the iron at Site III′, forming an octahedrally coordinated Fe^{3+} which could be responsible for the smaller quadrupole-split Fe^{3+} doublet.

CONCLUDING REMARK

Metal cations and associated ligands (e.g., O^{2-}) may be located at sites in Y zeolites which are not readily accessible to gases. For example, Fe^{2+} may be located at Site I in the hexagonal prisms and O^{2-} may be present as bridges between Fe^{2+} cations at Sites I′ and II′ in the sodalite cages. The limited accessibility of such species would normally hinder their direct participation in catalytic processes. However, the mobility of cations in the zeolite structure and the ability of adsorbed species to trap cations at sites of high accessibility in the structure provide a means by which these cations, and/or associated ligands, may still function as active sites for catalytic reactions. Such may be the case for the participation in redox reactions of iron cations at Site III′ in Fe–Y zeolite.

ACKNOWLEDGMENTS

One of us (C.Y.) wishes to acknowledge the financial support of the Peoples' Republic of China which afforded him the opportunity to be a visiting scholar at the University of Wisconsin–Madison. In addition, W.N.D. would like to thank the Department of Chemical Engineering at the University of Wisconsin–Madison for their hospitality during the sabbatical semester which enabled his participation in this work. Finally, all of us would like to acknowledge valuable discussions with Professor J. B. Uytterhoeven. This work was partly supported by a grant from the General Motors Research Laboratories.

REFERENCES

1. Delgass, W. N., Garten, R. L., and Boudart, M., *J. Phys. Chem.* **73,** 2970 (1969); Garten, R. L., Delgass, W. N., and Boudart, M., *J. Catal.* **18,** 90 (1970).
2. Fu, C. M., Deeba, M., and Hall, W. K., *Ind. Eng. Chem. Prod. Res. Dev.* **19,** 299 (1980).
3. Fu, C. M., Dorchak, V. N., and Hall, W. K., *J. Catal.* **68,** 166 (1981).
4. Pearce, J. R., Mortier, W. J., and Uytterhoeven, J. B., *J. Chem. Soc. Faraday Trans. I* **77,** 937 (1981).
5. Seiyama, T., Arakawa, T., Matsuda, T., Takita, Y., and Yamazoe, N., *J. Catal.* **48,** 1 (1977).
6. Chao, C., and Lunsford, J. H., *J. Amer. Chem. Soc.* **93,** 71 (1971).
7. Iizuka, T., and Lunsford, J. H., *J. Mol. Catal.* **8,** 391 (1980).
8. Jermyn, J. W., Johnson, T. J., Vansant, E. F., and Lunsford, J. H., *J. Phys. Chem.* **77,** 2964 (1973).
9. Lunsford, J. H., *in* "The Catalytic Chemistry of Nitrogen Oxides" (R. L. Klimisch and J. G. Larson, Eds.), p. 3. Plenum, New York, 1975.
10. Ballivet-Tkatchenki, D., and Coudurier, G., *Inorg. Chem.* **18,** 558 (1979).
11. Kasai, P. H., Bishop, R. J., Jr., and McLeod, D., Jr., *J. Phys. Chem.* **82,** 279 (1978).
12. Angell, C. L., and Schaffer, P. C., *J. Phys. Chem.* **70,** 1413 (1966); Rabo, J. A., Angell, C. L., Kasai, P. H., and Schomaker, V., *Discuss. Faraday Soc.* No. 41 328 (1966).
13. Ione, K. G., Romannikov, V. N., Davydov, A. A., and Orlova, L. B., *J. Catal.* **57,** 126 (1979).
14. Phillips, J., Clausen, B., and Dumesic, J. A., *J. Phys. Chem.* **84,** 1814 (1980).

15. Sørensen, K., Internal Report No. 1, Laboratory of Applied Physics II, Technical University of Denmark, Lyngby, Denmark, 1972.

16. Pearce, J. R., Sherwood, D. E., Hall, M. B., and Lunsford, J. H., *J. Phys. Chem.* **84,** 3215 (1980).

17. Shen, W. M., Dumesic, J. A., and Hill, C. G., Jr., *Rev. Sci. Instrum.* **52,** 858 (1981).

18. Enemark, J. H., and Feltham, R. D., *Coord. Chem. Rev.* **13,** 339 (1974).

19. Greenwood, N. N., and Gibb, T. C., "Mössbauer Spectroscopy," p. 91. Chapman & Hall, London, 1971.

20. Mortier, W. G., and Bosmans, H. G., *J. Phys. Chem.* **75,** 3327 (1971).